

Mass-Balancing of Electrodes as a Strategy to Widen the Operating Voltage Window of Carbon/Carbon Supercapacitors in Neutral Aqueous Electrolytes

Susana Vaquero¹, Jesus Palma¹, Marc Anderson^{1,2}, Rebeca Marcilla^{1,*}

¹ Electrochemical Processes Unit, IMDEA Energy Institute, E-28933, Mostoles (Madrid), Spain

² Environmental Chemistry and Technology Program, University of Wisconsin-Madison, WI, USA
53706

*E-mail: rebeca.marcilla@imdea.org

Received: 30 April 2013 / Accepted: 19 June 2013 / Published: 1 August 2013

In the present study, the effect of mass-balancing electrodes with respect to electrochemical performance of carbon-based supercapacitors (SCs) is investigated. It was found that by adjusting the mass ratio of positive and negative electrodes in SCs using the same active material in both electrodes (Pica activated carbon) one can extend the operating voltage of the SC beyond the typical window of stability for aqueous electrolyte systems. After studying the electrochemical stability window of single electrodes using cyclic voltammetry, symmetric (positive and negative electrode with the same mass) and asymmetric SCs (mass ratio of 2.46 positive / negative electrodes) are assembled and characterized. The results confirm that the asymmetric carbon-based SCs with mass ratio of 2.46 and a cycling history of 2000 cycles at 1.6 V and 5000 cycles more at 1.8 V, is able to retain over 75% of the initial capacitance after 7000 additional charge-discharge cycles at 2 V. On the contrary, a decreasing performance of the symmetric system losing more than 90% of the initial capacitance is detected under the same experimental conditions. Moreover, some insights about the electrochemical processes which occur during cycling of EDLCs are given. In particular, infrared spectroscopy experiments indicate that the loss of performance of symmetric carbon-based SC is dominated by the aging of the positive electrode.

Keywords: Activated carbon, electrochemical stability window, aging, mass-balancing, supercapacitor.

1. INTRODUCTION

Carbon-based supercapacitors (SCs) are very attractive electrochemical energy storage devices for a large number of applications [1, 2]. In most cases, they are used to deliver a very high power

during a short time. Unfortunately, the energy density delivered or stored in commercial carbon-based SCs is deficient as compared with conventional batteries. In order to increase the range of applications that could utilize these devices, most research activities have been oriented towards increasing their energy density. In this sense, and taking into account the following equation

$$E_{\max} = \frac{1}{2} CV^2 \quad (1)$$

that defines the maximum energy of a SC as a function of their capacitance (C) and operating voltage range, two approaches are considered: enhancing the intrinsic capacitance of the active materials or increasing the operating voltage of the system.

Regarding the first approach, capacitance of carbonaceous materials may be improved by pseudo-faradaic contributions related to charge transfer on active sites present at surface functional groups of these carbons [3-6]. This pseudocapacitance may also be provided by other type of electrode materials such as transition metal oxides [7, 8] and conducting polymers [9-12] that exhibit much higher theoretical capacitance than activated carbons.

The second approach consists of increasing operating voltage which depends on the electrochemical stability window of the electrolyte. The theoretical stability window of commonly used acid (1 M H₂SO₄) or basic (6 M KOH) aqueous electrolytes is about 1.2 V. As a consequence, the operating voltage for carbon-based SCs using these electrolytes is low (around 1 V). In contrast, most of the commercially available supercapacitors utilize organic electrolytes, allowing these SCs to reach voltages of about 2.7 V and consequently, higher values of energy density. Unfortunately, such electrolytes are quite expensive, ecologically unfriendly and require a complicated assembling process in comparison with aqueous electrolytes. Although the highest operating voltages are obtained with ionic liquids (ILs) (3.5 V approx.), these electrolytes are low in ionic conductivity and have high viscosities limiting the specific power and rate capability of these SCs especially at room temperature [13, 14]. Recently, it has been shown that SCs using activated carbon electrodes operating in neutral electrolytes have been able to achieve a wider electrochemical stability window due to the high cathodic overpotential for hydrogen evolution reaction observed at neutral pH [15, 16]. This feature, besides the fact that these aqueous neutral electrolytes are cheap, non-corrosive and environmentally friendly make these electrolytes very attractive for electrochemical capacitors.

Since the capacitance of activated carbon in neutral media is lower than in acidic or basic electrolytes, the use of neutral electrolytes has been mainly reserved to hybrid systems with metallic oxides [17] or conducting polymers [18] working as positive electrodes. The use of equation 2 to calculate the mass ratio in a hybrid supercapacitor allows the operating voltage range to be extended up to 2 V in neutral media [19].

$$\frac{m^+}{m^-} = \frac{C^- \Delta E^-}{C^+ \Delta E^+} \quad (2)$$

Where m^+ and m^- are the active mass and C^+ and C^- the specific capacitance for the positive and negative electrodes, respectively. ΔE^- and ΔE^+ are the potential difference from the open circuit voltage (OCV) to the negative and positive potential stability limits, respectively. This equation is widely used in literature for assembling hybrid supercapacitors with electrodes having different values

of specific capacitance ($C^- \neq C^+$) and/or operating at different voltage ($\Delta E^- \neq \Delta E^+$) [20]. However, this equation may be also applied to non-hybrid systems to increase the operating voltage of the supercapacitors. This strategy was successfully applied for the first time in ionic liquid (IL)-based supercapacitors reaching maximum cell voltage of 3.8 V instead of 3.5 V of symmetric SCs [21, 22]. Only very recently Chen *et al.* reported the effect of mass-balancing on the performance of SCs using the same activated carbon in both electrodes in neutral electrolyte [23]. It is worth mentioning that, from an economical point of view, the use of the same carbon material for both positive and negative electrodes requires simpler production processes as compared to that of the hybrid systems based on metal oxides, conducting polymers or ion insertion electrode materials.

In this study, we apply this mass-balancing strategy in supercapacitors working in neutral electrolyte having both positive and negative electrodes of the same activated carbon. This work complements the findings of Chen *et al.* with additional impedance spectroscopy analysis and extends the mass-balancing strategy to different kind of carbons. Moreover, we give some insights about the electrochemical processes which occur during cycling of supercapacitors. In particular, we try to correlate electrochemical behaviour of SC after severe cycling with the physicochemical changes undergone by their single electrodes.

2. EXPERIMENTAL

2.1 Electrode preparation

Commercial activated carbon Picatif BP 10 (Pica) provided by PICA was used as received. Polytetrafluoroethylene (PTFE 60 wt.% dispersion in water, Sigma Aldrich) was employed as a binder and acetylene black (Sigma Aldrich) used as a conductive agent for electrode preparation. As a standard procedure, a paste was prepared by vigorous mixing the activated carbon (70 wt.%), acetylene black (20 wt.%, Sigma Aldrich) and PTFE (10 wt.%, Sigma Aldrich) in 2-propanol. The paste was rolled onto a coin-shaped stainless steel mesh current collector ($d = 1\text{ cm}$). The electrodes were then pressed with a uniaxial press (CARVER model 3853-0) applying a pressure of 450 kg cm^{-2} and dried at room temperature overnight. The mass-loading of the dried electrodes was about 6 mg cm^{-2} .

2.2 Electrochemical set-up and supercapacitor assembly

Three types of cell configurations were used for performing the electrochemical characterization. Configuration 1 consists of a standard three electrode electrochemical cell using 0.5 M K_2SO_4 aqueous electrolyte, Pica carbon based electrode as the working electrode, platinum mesh as the counter and Ag/AgCl as reference electrode. Supercapacitors were built by assembling a cellulosic separator embedded with the neutral electrolyte (0.5 M K_2SO_4) between two Pica carbon electrodes in three-electrode Swagelok[®] cells (configuration 2) and in two-electrode Swagelok[®] cells (configuration 3). The only difference between symmetric and asymmetric SCs was the use of the same mass of active material in both electrodes ($m^+ = m^-$) for symmetric SCs and different mass ratios ($m^+ \neq m^-$) in

asymmetric SCs. It is worth mentioning that in some classifications of SCs asymmetric systems are considered supercapacitors with different kind of materials in positive and negative electrode (eg, MnO₂ and activated carbon). Nevertheless, this kind of system is named here hybrid capacitor while the term asymmetric is used for SCs having the same type of active material but different masses of materials comprising each electrode.

2.3 Electrochemical characterization techniques

The electrochemical stability window (ESW) was studied by cyclic voltammetry (CV) on the standard three electrode cell (configuration 1) at scan rates of 20 mV s⁻¹ and 2 mV s⁻¹, and varying the positive and negative potential limits.

Configuration 2 and 3 were used to characterize the electrochemical behaviour of the complete SCs. Three-electrode Swagelok[®] cells (configuration 2) were used to perform galvanostatic charge-discharge (CD) experiments applying a current density of 10 mA cm⁻² from 0 V to different cut-off voltages. This configuration allows for the monitoring of electrochemical behaviour for the complete system while also recording separately the individual positive and negative electrode potentials [24].

A two-electrode Swagelok (configuration 3) was used to study the cyclability of SCs that was followed by galvanostatic charge-discharge (CD) experiments carried out at 10 mA cm⁻² from 0V to different cut-off voltages; 1.6, 1.8 and 2 V during a high number of cycles. Impedance spectroscopy experiments were also performed using this configuration. The frequency range studied varied from 200 kHz to 10 mHz at bias voltage of 0 V with a potential amplitude of 10 mV.

Specific capacitance (C_{SC}), equivalent series resistance (ESR) and the specific real energy (E_{real}) of the SCs were calculated from CD experiments by applying equations 3-5 to the discharge profile.

$$C_{SC}(\text{F g}^{-1}) = \frac{I}{m_{tam} \cdot (dV/dt)} \quad (3)$$

$$ESR(\Omega \text{ cm}^2) = \frac{\Delta V \cdot A}{2 \cdot I} \quad (4)$$

$$E_{real}(\text{Wh kg}^{-1}) = \frac{1}{m_{tam}} \int_{t_i}^{t_f} I \cdot V \cdot dt = \frac{I}{m_{tam}} \int_{t_i}^{t_f} V dt \quad (5)$$

Where I is the discharge current, m_{tam} is the total active mass in the SC, dV/dt is the slope of the discharge curve, ΔV is the ohmic drop when current is reversed and A is the geometric area of the electrodes. t_i and t_f are the integration limits corresponding to the time in which the discharge starts and finishes, respectively.

2.4 Fourier Transform Infrared Spectroscopy (FTIR)

The FTIR spectra of electrodes were recorded using a Thermo NICOLET 6700 equipment operating in diffuse reflectance mode (DRIFT).

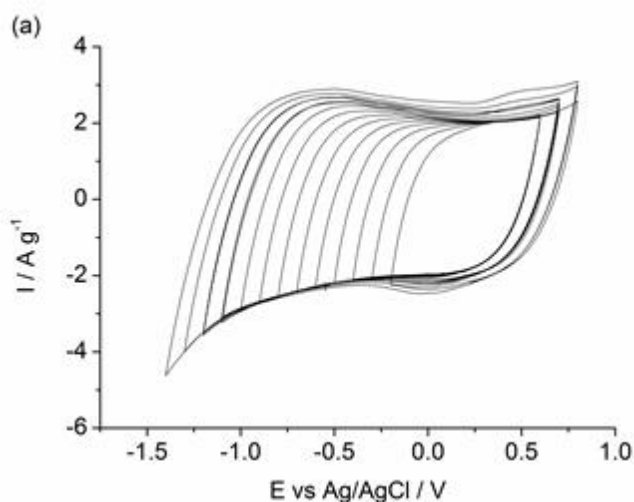
The FTIR spectrum was collected after 128 scans at a resolution of 4 cm^{-1} in the range of $4000\text{--}650\text{ cm}^{-1}$.

3. RESULTS AND DISCUSSION

A detailed physicochemical characterization of the activated carbon (Pica) can be found elsewhere [25]. In brief, Pica carbon exhibits micro-meso porosity with a percentage of micropore volume (V_{micro}) of 48 % and a specific surface area (S_{BET}) of $2411\text{ m}^2\text{ g}^{-1}$. Presence of functional groups is less than 2% in weight (determined by thermogravimetric analysis).

In order to investigate the electrochemical stability window (ESW) of $0.5\text{ M K}_2\text{SO}_4$ aqueous electrolyte in combination with Pica carbon, cyclic voltammetry experiments were performed in a standard three electrode cell (configuration 1). An open circuit voltage (OCV) of 0.18 V vs. Ag/AgCl was measured before performing CVs by following the evolution of potential with time until voltage stabilization. Fig. 1a shows the cyclic voltammetry of Pica electrode in $0.5\text{ M K}_2\text{SO}_4$ aqueous electrolyte at scan rate of 20 mV/s , where the positive and negative potential were extended during the experiment. Quasi-rectangular shape of CV can be observed for narrow potential windows indicating pure capacitive behaviour. The rectangular shape of the CV begins to become distorted when the positive and negative potentials are enlarged. Although it is difficult to establish the electrochemical stability window categorically, -1.1 V and 0.7 V were determined as potential limits since the coulombic efficiency is higher than 95 % within this range (considered as the threshold of reversibility). Depending on operating conditions, the potential window might reach to 2 V . Beyond these potential limits current increases quickly indicating the presence of faradaic reactions with the electrolyte.

In order to confirm these potential limits, CV was performed in $0.5\text{ M K}_2\text{SO}_4$ between -1.1 V and 0.7 V at a lower scan rate of 2 mV s^{-1} (see Fig. 1b). Coulombic efficiency of the system under this more restrictive scan rate is 96 %, still higher than 95 %.



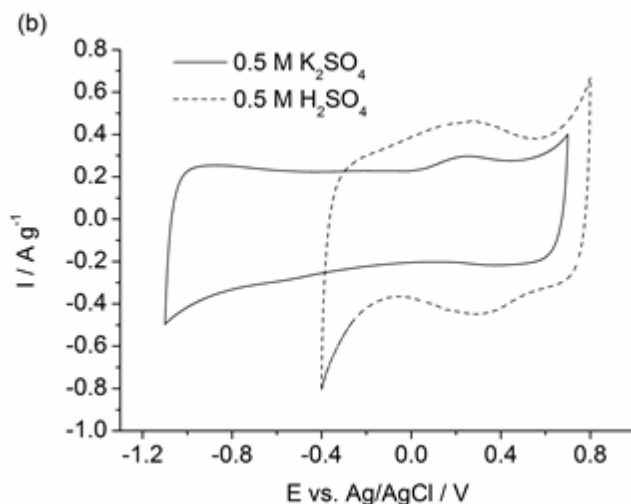


Figure 1. CVs of a three electrode cell in 0.5 M K_2SO_4 aqueous electrolyte (a) at scan rate of 20 mV s^{-1} and different positive and negative potential limits and (b) CVs at 2 mV s^{-1} in 0.5 M K_2SO_4 (—) and 0.5 M H_2SO_4 (···).

Moreover, the CV of Pica carbon in acidic electrolyte (0.5 M H_2SO_4) was also performed for purposes of comparison (Fig. 1b). In the case of acidic electrolytes, a narrower potential window of 1.2 V was found with -0.4 V and 0.8 V as negative and positive limits, respectively. The overpotential for di-hydrogen evolution in neutral media was attributed to the storage of nascent hydrogen in activated carbon below the thermodynamic potential for water decomposition [26]. The hump at 0.25 V during the anodic scan was already observed by Béguin in 0.5 M Na_2SO_4 and was associated to the electro-oxidation of hydrogen being trapped in the pores of activated carbon at negative potentials [15].

Although CVs in three electrode configuration suggest that a supercapacitor using Pica carbon as active material and 0.5 M K_2SO_4 as electrolyte should be capable of operating to $\sim 1.8 - 2 \text{ V}$, this has been demonstrated to be not straightforward. The main reason is that carbon-based SCs have been traditionally fabricated using electrodes of the same mass of carbon in both positive and negative electrodes. This means that Eq. (2) is rarely considered in constructing these SCs. However, in a carbon-based SC, having two electrodes composed of the same active material ($C^- = C^+$) the potential window of the two electrodes is not always the same. This is particularly true in neutral electrolytes displaying a cathodic overpotential for hydrogen evolution where the potential window of the negative electrode is significantly wider than the positive window ($\Delta E^- > \Delta E^+$). Therefore, if the same mass of active materials is used in both electrodes to assemble a symmetric SC, the maximum operating voltage of the SC will be reached as soon as the positive electrode achieves its potential stability limit. The potential of the negative electrode will be still far away from any limiting degradation potential. As a consequence, the available potential window of the active material/neutral electrolyte combination will not be fully utilized. In this work, we have utilized Eq. (2) in calculating the optimum mass ratio (m^+/m^-) by which to assemble SCs. Due to the rectangular voltammetry with comparable positive and negative currents over the entire voltage window (Fig. 1), it could be assumed that specific capacitance of Pica is similar towards positive and negative potentials ($C_{am}^- \approx C^+ \approx C^-$). Therefore, Eq. (2) is simplified to the following expression: $m^+/m^- = \Delta E^- / \Delta E^+$. Taking into account the OCV and the potential limits established by CV, $\Delta E^- = 1.28 \text{ V}$ and $\Delta E^+ = 0.52 \text{ V}$, the value of m^+/m^-

was calculated to be 2.46. In order to validate this mass ratio, three-electrode Swagelok[®] cells including Ag/AgCl reference electrode (configuration 2) were assembled for symmetric SCs and asymmetric SCs. In symmetric SCs, the mass of active mass in both electrodes was identical ($m^+/m^- = 1$) whereas in asymmetric SCs the mass of active material in both electrodes was balanced ($m^+/m^- = 2.46$). Figures 2a and 2b show galvanostatic charge-discharge profiles at a discharge current density of 10 mA cm⁻² from 0 V to different cut-off voltages (1.4, 1.6 and 1.8 V) for symmetric and asymmetric systems, respectively.

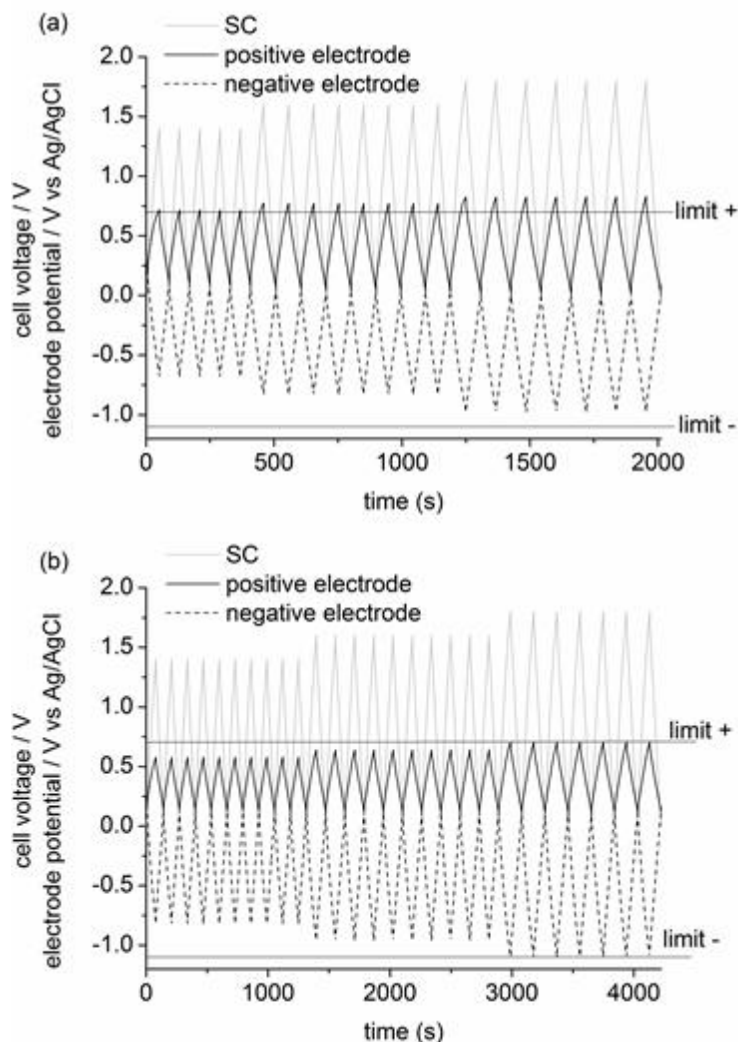


Figure 2. Galvanostatic charge-discharge curves ($I=10$ mA cm²) of the Pica SCs in 0.5 M K₂SO₄ aqueous electrolyte at cut-off voltages of 1.4, 1.6 and 1.8 V. Individual electrode potential profiles are also shown. a) Symmetric system ($m^+/m^- = 1$) and (b) Asymmetric system ($m^+/m^- = 2.46$)

The horizontal lines represent the potential stability limits determined by CV measurements (-1.1 V and 0.7 V). SCs profiles in both Figures display typical triangular shapes indicating the absence of significant faradaic reactions over the voltage ranges studied. Individual voltage profiles in Fig. 2a show that positive electrode is much closer to its corresponding voltage limit than that of the negative

electrode. Even at 1.4 V (the lowest cut-off potential), the positive electrode approaches its potential limit whereas the negative electrode remains a long voltage away from its limit. At 1.8 V, the positive electrode further exceeded its potential limit while the negative electrode remained within its limit of stability. As a consequence, the high hydrogen overpotential of Pica in 0.5 M K_2SO_4 cannot be fully exploited with respect to achieving high operating cell voltages in symmetric cells. Fig. 2b shows that in an asymmetric system, with mass-balanced electrodes, it was possible to maintain individual voltage profiles of positive and negative electrodes inside their corresponding limits even at 1.8 V.

These results indicate that asymmetric SCs are expected to exhibit better performance at higher cut-off potentials than their symmetric SC counterparts. To corroborate these assumptions, symmetric and asymmetric SCs were assembled in conventional two-electrode Swagelok[®] cells (configuration 3) to perform cycle life testing. Complete charge-discharge cycles at 10 mA cm^{-2} were performed from 0V to 1.6 V and back to 0V over 2000 cycles followed by an increase in the operating voltage up to 1.8 V conducted for 5000 more cycles. Lastly, we cycled the system for 7000 more times after increasing the operating voltage to 2 V.

Specific capacitance (C_{SC}), equivalent series resistance (ESR) and the specific real energy (E_{real}) of the supercapacitors were calculated from CD experiments by applying equations 3-5 to the discharge profiles. By using Eq. (6) and taking into account the following considerations; $C_{am} \approx C^+ \approx C^-$, $m_{tam} = m^+ + m^-$, Eq. (7) was obtained.

$$C_{am} = \frac{m_{tam}^2}{m_- \cdot m_+} C_{SC} \quad (6)$$

$$\frac{1}{m_{tam} C_{SC}} = \frac{1}{m^+ C^+} + \frac{1}{m^- C^-} \quad (7)$$

Resulting that:

$C_{am} = 4C_{SC}$ for symmetric SCs ($m^+ / m^- = 1$) and

$C_{am} = 4.87 \cdot C_{SC}$ for asymmetric SCs when $m^+ / m^- = 2.46$.

Fig. 3 shows the evolution of the specific capacitance of Pica active material (C_{am}) in both symmetric and asymmetric SCs over 14000 cycles when cycled consecutively at 1.6, 1.8 and 2 V. Similar specific capacitances (C_{am}) of Pica carbon were obtained when increasing the cut-off voltage in both systems. A small decrease in C_{am} is observed for the symmetric SC after 2000 cycles at 1.6 V ($\sim 6\%$). When cut-off voltage was increased to 1.8 V an initial C_{am} enhancement was observed followed by a fade of $\sim 8\%$. In contrast, no capacitance fade was observed for the asymmetric SC neither at 1.6 V nor 1.8 V. Finally, cut-off voltage was increased up to 2 V. Although C_{am} for the symmetric system remained steady for 3000 cycles (10000 cycles in total), further cycling resulted in a significant decrease. After 7000 cycles at 2 V (14000 in total) C_{am} experienced a fade of around 90% for the symmetric system whereas the asymmetric system retained more than 75% of their initial C_{am} value at

2 V. This represents further evidence of the better performance of asymmetric or mass-balanced SCs in 0.5 M K₂SO₄ aqueous electrolyte.

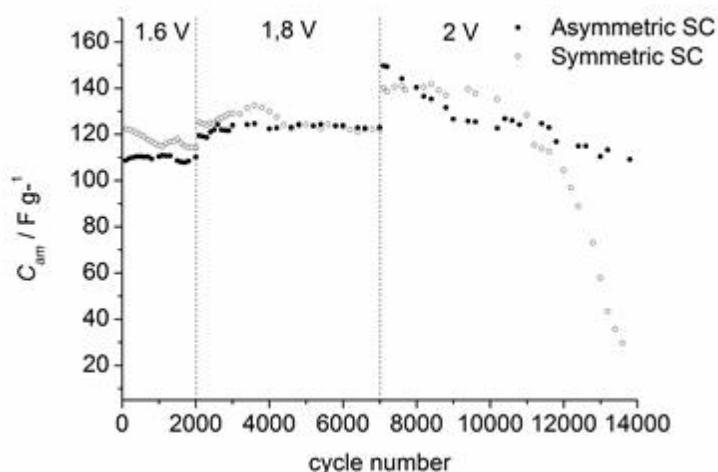


Figure 3. Specific capacitance (C_{am}) of symmetric and asymmetric SCs in 0.5 M K₂SO₄ aqueous electrolyte vs. the number of cycles. Discharge current density $I = 10\ mA\ cm^{-1}$, cut-off voltages $V_{max} = 1.6\ V, 1.8\ V$ and $2\ V$.

Fig. 4 shows the evolution of the real energy (E_{real}) with the number of charge-discharge cycles. At 1.6 V the specific energy values were determined to be $9.3\ Wh\ kg^{-1}$ and $7.3\ Wh\ kg^{-1}$ during the first cycles for the symmetric and asymmetric system, respectively. No significant energy decay was observed after 2000 cycles.

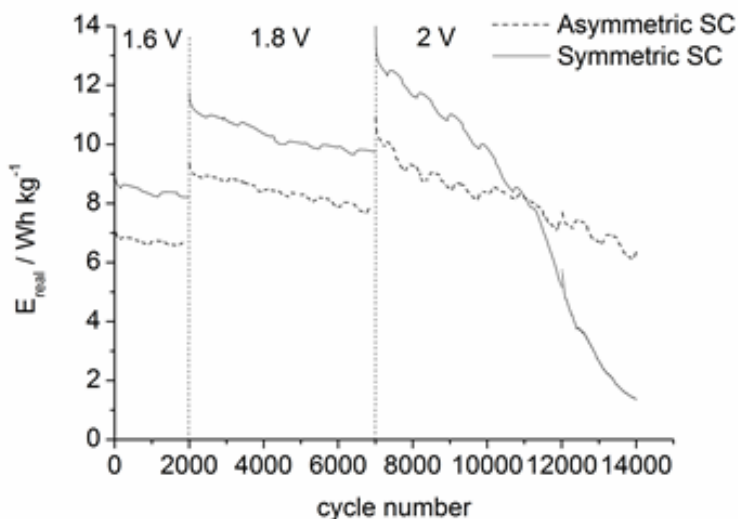


Figure 4. Specific real energy (E_{real}) of symmetric and asymmetric SCs in 0.5 M K₂SO₄ aqueous electrolyte vs. the number of cycles. $I = 10\ mA\ cm^{-1}$, $V_{max} = 1.6\ V, 1.8\ V$ and $2\ V$.

As expected, when cut-off voltage was increased to 1.8 V, the specific energy increased for both systems; 11.6 Wh kg⁻¹ for the symmetric SC and 9.3 Wh kg⁻¹ for the asymmetric SC. After 5000 cycles at 1.8 V the E_{real} decreased less than 15 % in both SCs. As shown in Fig. 4. this energy fade became much more noticeable when the cut-off voltage was increased to 2 V, especially for the symmetric SC. In that case, the energy dropped drastically from 13 Wh kg⁻¹ to 1 Wh kg⁻¹ (> 90 %), whereas for the asymmetric system it decreased only from 10.3 to 6.3 Wh kg⁻¹ (< 40 %). The fluctuations observed in E_{real} could be likely attributed to the change of temperature in the laboratory occurring due to diurnal fluctuations.

Fig. 5 depicts the evolution of equivalent series resistance (ESR) of both symmetric and asymmetric SCs. It is observed from Fig. 5 that ESR values are only slightly different for both systems at 1.6 and 1.8 V, being 1 Ω cm² for the asymmetric SC and in the range of 1-1.5 Ω cm² for the symmetric SC. However, at 2 V it is clearly observed that ESR values for the symmetric SC drastically increased reaching a value of 9 Ω cm² at cycle 14000, whereas a maximum value of 2.5 Ω cm² was found for the asymmetric SC. The evolution of ESR with cycle number correlates well with the tendency followed by specific capacitance (C_{am}) and specific real energy (E_{real}).

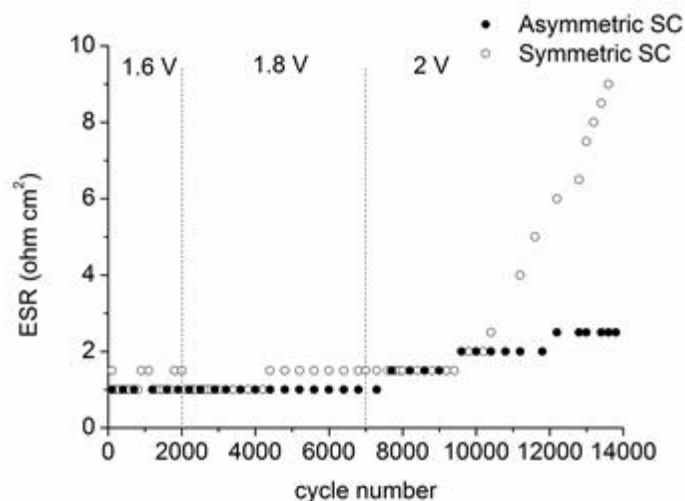


Figure 5. Equivalent Series Resistance (ESR) of symmetric and asymmetric SCs in 0.5 M K₂SO₄ aqueous electrolyte vs. the number of cycles. $I = 10$ mA cm⁻¹, $V_{max} = 1.6$ V, 1.8 V and 2 V.

Fig. 6 depicts the voltage profiles of both symmetric and asymmetric SCs when cycled to 2 V after different number of cycles. It is worth mentioning that voltage profiles obtained at 1.6 V and 1.8 V were linear and showed symmetric characteristics, confirming a pure capacitive behaviour for both symmetric and asymmetric SCs. In Fig. 6a we can see that in cycle 8000 (only after 1000 cycles at 2 V) voltage profiles of both systems are quite similar showing a capacitive behaviour. This correlates well with the high capacitance (C_{am}) and energy values (E_{real}) and with the low ESR exhibited by the two SCs at that point of cycling.

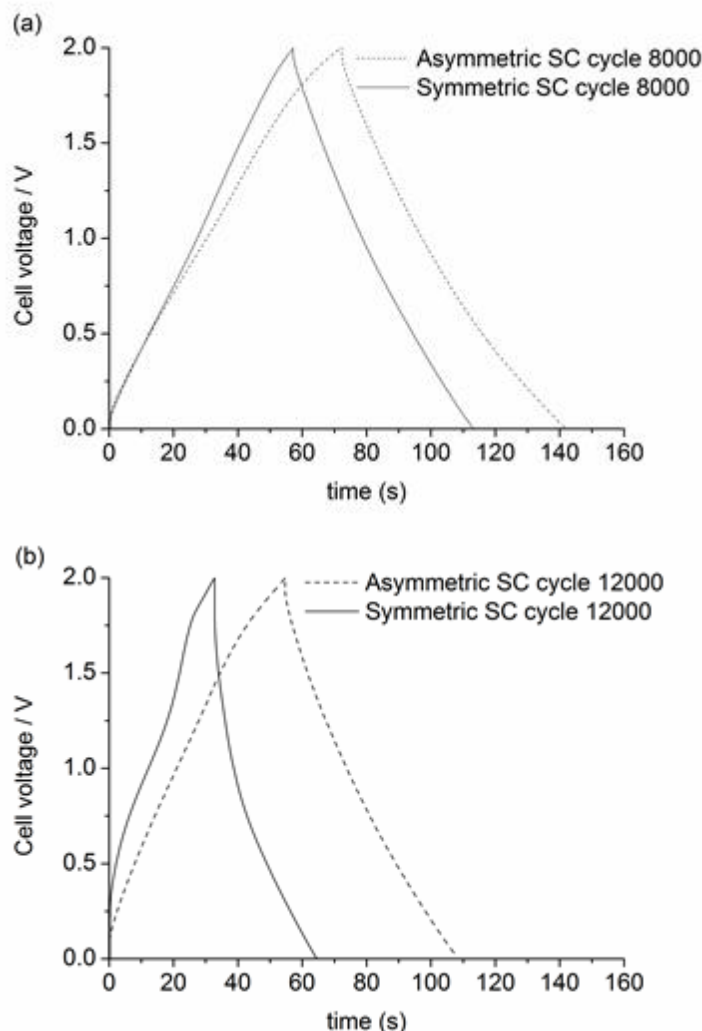


Figure 6. Galvanostatic charge-discharge profiles ($I=10 \text{ mA cm}^2$) of symmetric and asymmetric SCs in $0.5 \text{ M K}_2\text{SO}_4$ aqueous electrolyte (a) after 8000 cycles and (b) after 12000 cycles.

Fig. 6b shows the voltage profiles of both SCs at cycle 12000 (after 5000 cycles at 2 V). At that moment, the voltage profile of the symmetric SCs deviates significantly from linearity whereas a linear triangular shape corresponding to double layer capacitive behaviour was observed for the asymmetric SC. The degradation of the symmetric SC after 12000 cycles was evidenced by the completely distorted charge-discharge profile being in good agreement with the poor electrochemical performance exhibited by the symmetric SC and represented in Figs. 3, 4 and 5. On the contrary, the linear voltage profile of asymmetric SC demonstrated no significant degradation after 12000 cycles for that system.

In order to follow the behaviour of the symmetric and asymmetric SCs during the charge-discharge experiments, several impedance experiments were performed; before cycling, after 2000 cycles at 1.6 V, after 7000 cycles (2000 at 1.6 V and 5000 at 1.8 V) and finally after 12000 cycles (2000 at 1.6 V, 5000 at 1.8 V and 5000 at 2 V). Fig. 7a and Fig. 7b show Nyquist plots of symmetric and asymmetric SCs obtained at the same state of cycling. At very high frequencies, the imaginary part of the impedance tends to zero and the resistance measured is mainly determined by the electrolyte

(R_e). At high frequencies, the presence of a semi-circle is observed in both symmetric and asymmetric SCs. The diameter of this semi-circle has been described elsewhere as a pseudo-transfer resistance (R_i) and is associated with the porous structure of the electrode and with the presence of surface functional groups [27, 28]. The sum of both resistances (R_e+R_i) is related with the equivalent series resistance (ESR) obtained also from the charge-discharge experiments. At low frequencies, pure capacitive materials show a vertical line in Nyquist plot whereas the presence of diffusive effects results in a tilted line reaching an angle of 45° for pure diffusive behaviour.

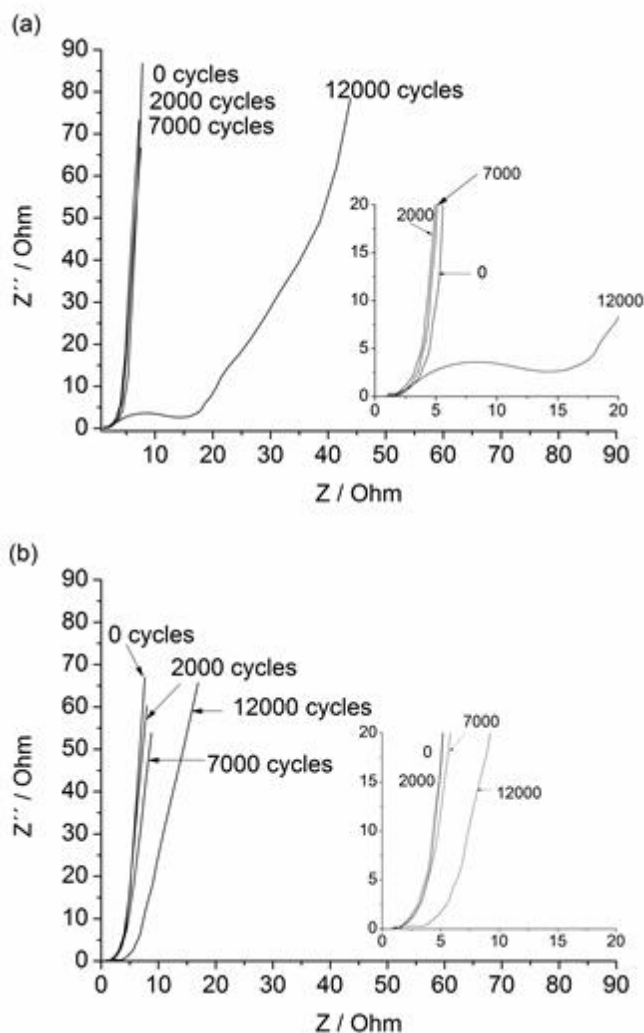


Figure 7. Nyquist plot of a) symmetric and b) asymmetric SCs in 0.5 M K_2SO_4 aqueous electrolyte after 0, 2000, 7000 and 12000 cycles.

In Fig. 7a Nyquist plots of symmetric SC after 2000 and 7000 cycles were very similar to the one for the freshly prepared SC ($ESR \approx 1-1.5 \Omega \text{ cm}^2$) indicating no important changes in the electrode surface of the SC after that period of cycling. However, the Nyquist plot of the symmetric SC after 12000 cycles shows a large semicircle corresponding to a huge ESR of $13 \Omega \text{ cm}^2$ also evidenced by galvanostatic charge-discharge experiments. Furthermore, a line tilted about 45° appears in the Nyquist

plot of symmetric SC after 12000 cycles showing that the diffusive contribution to the impedance is more important. The high resistance of symmetric SC can be attributed to increased contact resistances, which may occur between individual grains within the electrode, between the electrode and the current collectors, or to an increased distributed resistance within the porous microstructure. In the full cell impedance study by Ishimoto et al. [29] with organic electrolyte, the latter resistance contribution was found to be the clearly dominant term. Impedance spectroscopy results point to a similar hypothesis for the neutral aqueous electrolyte because the *ESR* increase is due to an increase in the diameter of the semicircle that is associated mainly with the porous structure of the electrode.

Fig. 7b shows the Nyquist plots of the asymmetric SC. Nyquist plot of a freshly fabricated SC and after 2000 and 7000 cycles were very similar with *ESR* values between 1-1.5 $\Omega \text{ cm}^2$, also similar to the values obtained for the symmetric SC. However, although Nyquist plot of the asymmetric SC after 12000 also showed an increase of *ESR*, this increase is much less pronounced than in the case of the symmetric SC (2.5 $\Omega \text{ cm}^2$ vs. 13 $\Omega \text{ cm}^2$). These results are in good agreement with the galvanostatic charge-discharge experiments and corroborate the hypothesis that major electrode degradation is likely occurring in the symmetric SC.

As mentioned before, the positive electrode of a symmetric SC is working beyond its voltage limit of stability while the negative electrode is still far from reaching its negative limit. This suggests that the aging of symmetric SCs is dominated by the degradation of positive electrode. In order to further test this assumption a “post mortem” FTIR spectra of both positive and negative electrodes of the symmetric SC after 14000 cycles were performed (Fig. 8). It is worth mentioning that although there are several studies devoted to investigating the causes of aging in organic electrolytes [30-32] the aging in neutral electrolytes has not been reported in detail.

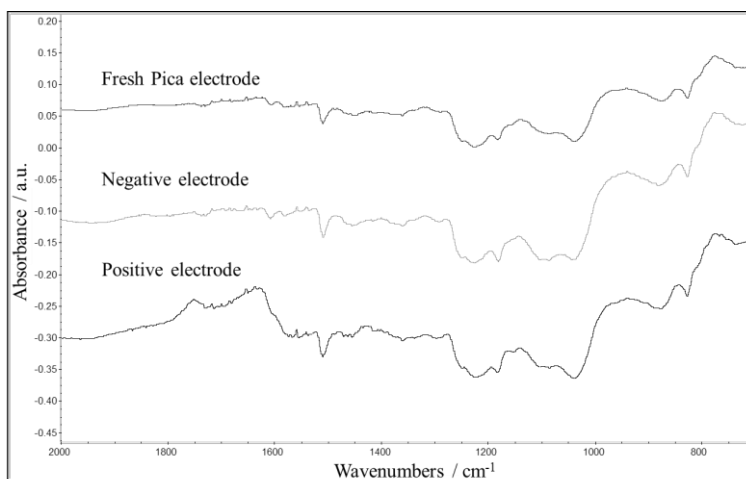


Figure 8. FTIR spectra of fresh Pica electrode and “post mortem” negative and positive electrodes of symmetric SC.

Fig. 8 shows that the FTIR spectrum of the negative electrode is very similar to the spectrum of a fresh Pica electrode. No chemical changes associated with new bands appear even after severe cycling. However, new intense and broad bands centred around 1750-1638 appear in the FTIR spectra

of the positive electrode. The vibration at 1750 cm^{-1} might result of several C=O absorptions due to the creation of oxygenated functional groups. In particular, this vibration indicates that ester groups or larger lactones, which absorb in the same range as open-chain esters dominate the spectrum. Appearance of quinoidal carbonyl groups in the positive electrode is supported by the new vibration centred at 1638 cm^{-1} [33].

A small band at 1438 cm^{-1} can be assigned to C-O-H bending in carboxylic acids and phenols and also to C-H deformations and even to aromatic C=C stretch [32]. Other small peaks such as the bands at 1249-1167 can be attributed to C-O stretching and O-H bending modes in either lactone, carboxyl and phenolic structures respectively. All these new bands were created as a process of aging in the symmetric SC when this is cycled beyond its maximum operating voltage. These FTIR results provide additional evidence that the electrochemical performance decay of SCs in neutral electrolyte is mainly caused by the degradation of positive electrode. Appearance of organic species in this electrode might be a consequence of electrolyte degradation and carbon oxidation processes at positive potentials.

4. CONCLUSION

The beneficial effect of mass-balancing electrodes with respect to the electrochemical behaviour of carbon-based supercapacitors with neutral electrolyte was investigated in detail. Cyclic voltammetry studies in 0.5 M K_2SO_4 provided evidence as to the wide electrochemical stability window of this electrolyte with electrodes made of Pica activated carbon. Those results were used to estimate the theoretical mass ratio of active material that was found to be $m^+/m^- = 2.46$. Asymmetric supercapacitors assembled by using this mass ratio besides symmetric supercapacitor with $m^+/m^- = 1$ were assembled and electrochemically characterized by charge-discharge and impedance spectroscopy. Although both symmetric and asymmetric SCs exhibited a good performance after 7000 cycles at 1.8 V, the complete fading of the performance of symmetric SC occurred when voltage increased to 2 V. In contrast, the behaviour of the asymmetric SC was much better in terms of retention of specific energy, capacity and equivalent series resistance. We have demonstrated the benefits of using an asymmetric design for extending the operation voltage in a neutral aqueous electrolyte. Moreover, results obtained from “post mortem” infrared spectroscopy showed the presence of degradation products only for the positive electrode. This confirmed that the performance fading of the symmetric SC in neutral electrolyte is mainly due to the degradation of positive electrode, which is the one that exceeds the limit of stability with respect to voltage in non-balanced symmetric configurations.

This method of mass-balancing electrodes should be used not only for neutral electrolytes but should become a common routine for designing SCs with other electrolytes in which the positive and negative electrodes show non-symmetrical behavior such as in organic and ionic liquid-based electrolytes. This work is in progress in our lab and will be presented in a next article.

ACKNOWLEDGEMENT

R.M. acknowledges financial support from the MINECO (former MICINN) through the Ramón y Cajal Program (RYC-2011-08093) and ENE2012-31516 Project.

References

1. B.E. Conway, *Electrochemical supercapacitors: scientific fundamentals and technological applications*, Plenum Pub Corp, 1999.
2. P. Simon, Y. Gogotsi, *Nat. Mater.*, 7 (2008) 845-854.
3. V. Khomenko, E. Raymundo-Pinero, F. Beguin, *J. Power Sources*, 195 (2010) 4234-4241.
4. E.J. Ra, E. Raymundo-Pinero, Y.H. Lee, F. Beguin, *Carbon*, 47 (2009) 2984-2992.
5. M.J. Bleda-Martinez, J.A. Macia-Agullo, D. Lozano-Castello, E. Morallon, D. Cazorla-Amoros, A. Linares-Solano, *Carbon*, 43 (2005) 2677-2684.
6. D. Pech, D. Guay, T. Brousse, D. Belanger, *Electrochem. Solid St.*, 11 (2008) A202-A205.
7. T. Brousse, M. Toupin, D. Belanger, *J. Electrochem. Soc.*, 151 (2004) A614-A622.
8. T. Brousse, P.-L. Taberna, O. Crosnier, R. Dugas, P. Guillemet, Y. Scudeller, Y. Zhou, F. Favier, D. Belanger, P. Simon, *J. Power Sources*, 173 (2007) 633-641.
9. A. Laforgue, P. Simon, J.F. Fauvarque, J.F. Sarrau, P. Lailier, *J. Electrochem. Soc.*, 148 (2001).
10. M. Mastragostino, C. Arbizzani, F. Soavi, *Solid State Ionics*, 148 (2002).
11. C. Peng, S. Zhang, D. Jewell, G.Z. Chen, *Prog. Nat. Sci.*, 18 (2008) 777-788.
12. G.A. Snook, P. Kao, A.S. Best, *J. Power Sources*, 196 (2011) 1-12.
13. A. Balducci, R. Dugas, P.L. Taberna, P. Simon, D. Plee, M. Mastragostino, S. Passerini, *J. Power Sources*, 165 (2007) 922-927.
14. M. Mora Jaramillo, A. Mendoza, S. Vaquero, M. Anderson, J. Palma, R. Marcilla, *RSC Adv.*, 2 (2012).
15. L. Demarconnay, E. Raymundo-Pinero, F. Beguin, *Electrochem. Commun.*, 12 (2010) 1275-1278.
16. K. Fic, G. Lota, M. Meller, E. Frackowiak, *Energy Environ. Sci.*, 5 (2012) 5842-5850.
17. V. Khomenko, E. Raymundo-Pinero, E. Frackowiak, F. Beguin, *Appl. Phys. A-Mater.*, 82 (2006) 567-573.
18. C. Peng, S. Zhang, X. Zhou, G.Z. Chen, *Energy Environ. Sci.*, 3 (2010) 1499-1502.
19. V. Khomenko, E. Raymundo-Pinero, F. Beguin, *J. Power Sources*, 153 (2006) 183-190.
20. L. Demarconnay, E. Raymundo-Pinero, F. Beguin, *J. Power Sources*, 196 (2011) 580-586.
21. M. Lazzari, F. Soavi, M. Mastragostino, *J. Power Sources*, 178 (2008) 490-496.
22. M. Lazzari, F. Soavi, M. Mastragostino, *Fuel Cells*, 10 (2010) 840-847.
23. J.H. Chae, G.Z. Chen, *Electrochim. Acta*, 86 (2012) 248-254.
24. W.G. Pell, B.E. Conway, *J. Power Sources*, 136 (2004) 334-345.
25. S. Vaquero, R. Díaz, M. Anderson, J. Palma, R. Marcilla, *Electrochim. Acta*, 86 (2012) 241-247.
26. K. Jurewicz, E. Frackowiak, F. Beguin, *Appl. Phys. A-Mater.*, 78 (2004) 981-987.
27. J. Gamby, P.L. Taberna, P. Simon, J.F. Fauvarque, M. Chesneau, *J. Power Sources*, 101 (2001) 109-116.
28. Y.R. Nian, H.S. Teng, *J. Electroanal. Chem.*, 540 (2003) 119-127.
29. S. Ishimoto, Y. Asakawa, M. Shinya, K. Naoi, *J. Electrochem. Soc.*, 156 (2009) A563-A571.
30. P.W. Ruch, D. Cericola, A. Foelske, R. Koetz, A. Wokaun, *Electrochim. Acta*, 55 (2010) 2352-2357.
31. P. Azais, L. Duclaux, P. Florian, D. Massiot, M.A. Lillo-Rodenas, A. Linares-Solano, J.P. Peres, C. Jehoulet, F. Beguin, *J. Power Sources*, 171 (2007) 1046-1053.
32. A.M. Bittner, M. Zhu, Y. Yang, H.F. Waibel, M. Konuma, U. Starke, C.J. Weber, *J. Power Sources*, 203 (2012) 262-273.
33. J. Gulyas, E. Foldes, A. Lazar, B. Pukanszky, *Comp. Part a-Appl. S.*, 32 (2001) 353-360.